arXiv:1504.05280v1 [cond-mat.mes-hall] 21 Apr 2015

# Off-resonant polarized light-controlled thermoelectric transport in ultrathin topological insulators

M. Tahir† and P. Vasilopoulos⋆
*Concordia University, Department of Physics, 7141 Sherbrooke Ouest, Montréal, Québec, Canada, H4B 1R6*

We study thermoelectric transport in ultrathin topological insulators under the application of circularly polarized *off-resonant light* of frequency $\Omega$ and amplitude $A$. We derive analytical expressions for the band structure, orbital magnetization $M_{orb}$, and the thermal ($\kappa_{xy}$) and Nernst ($\alpha_{xy}$) conductivities. Reversing the light polarization from right to left leads to an exchange of the conduction and valence bands of the symmetric and antisymmetric surface states and to a sign change in $M_{orb}$, $\alpha_{xy}$, and $\kappa_{xy}$. Varying the sample thickness or $A/\Omega$ leads to a strong enhancement of $M_{orb}$ and $\alpha_{xy}$. These effects, accessible to experiments, open the possibility for selective, state-exchanged excitations under light and the conversion of heat to electric energy.

PACS numbers: 03.65.Vf, 72.15.Jf, 73.43.Nq, 85.75.-d

*Introduction.* Topological insulators (TIs) are insulators in the bulk but possess gapless surface states [1]. Due to their potential applications a wide variety of TIs has been found to be three dimensional and among them $Bi_2Se_3$ and $Bi_2Te_3$ are demonstrated as prototypes with single Dirac-cone surface states due to the strong spin-orbit interaction (SOI) [2–6]. By reducing their thickness to 6 nm or less, a finite hybridization occurs of their top and bottom surface states [3, 7] and has been realized in transistors [8]. Ultrathin TIs are promising materials for high performance optoelectronic devices, such as photodetectors [7] and transparent electrodes [9], and excellent thermoelectric materials [10, 11].

Berry-curvature mediated thermoelectric effects, generated by a temperature gradient [12], have been proposed for two-dimensional (2D) systems and explained related experiments very well [13]. Among their properties, the orbital magnetic moment and corresponding orbital magnetization [14, 15], and the thermal and Nernst conductivities [16–19] have attracted considerable attention. Also, Berry-curvature mediated transverse heat transport on the surface of TIs attached to a ferromagnet has been demonstrated [11] despite the complicated nature of the experiments. Of particular interest is the control of thermoelectric effects through the surface states of TIs under circularly polarized *off-resonant light* [20].

In recent years light-induced quantum effects have generated a strong interest, in particular quantum phase transitions in Floquet TIs driven by external time-periodic perturbations [21]. For such systems it is convenient to use Floquet theory proposed [20] recently for periodically driven graphene and TIs. In the appropriate frequency regime the off-resonant light cannot generate real photon absorption or emission due to energy conservation. Accordingly, it does not directly excite electrons but instead modifies the electron band structure through second-order virtual-photon absorption processes. When averaged over time, these processes result in an effective static alteration of the band gap of the system.

Floquet bands were first realized in photonic crystals [22] and have been verified by recent experiments on surfaces of TIs [23, 24]. However, nontrivial phase transitions, induced by *off-resonant light* on the surface states of ultrathin TIs, and the effect of this light on transport properties is an open question as it is not yet studied and is different than many optical effects in TI films [25]. In this work we partly answer this question by evaluating the band structure, orbital magnetization, and the thermal and Nernst conductivities of such TIs. Reversing the polarization of this light leads to an exchange of the conduction and valence bands of the symmetric and antisymmetric surface states and a tunable band gap. The details are as follows.

*Basic Formalism.* We consider surface states of ultrathin TIs in the (x,y) plane in the presence of circularly polarized light and hybridization between the top and bottom surface states. We first extend the 2D Dirac type Hamiltonian [7] by including a time-periodic field [20] as

$$H(t) = v_F(\sigma_x\Pi_y(t) - \sigma_y\Pi_x(t)) + s\Delta_h\sigma_z. \qquad (1)$$

Here $s = \pm 1$ for symmetric and antisymmetric combinations of the two surface states, ($\sigma_x$, $\sigma_y$, $\sigma_z$) are the Pauli matrices, $v_F$ the Fermi velocity, and $\Delta_h$ the hybridization energy between the top and bottom surface states that, depending on the thickness, varies from 41 meV to 250 meV [3, 7]. For simplicity we disregard higher order terms in $k$ since their contribution is very small and doesn't affect the major physics discussed below [26–28]. Further, $\mathbf{\Pi(t)} = \mathbf{P} + e\mathbf{A(t)}$ is the canonical momentum with vector potential $\mathbf{A}(t) = (lA\sin(\Omega t), A\cos\Omega t)$, $\mathbf{E}(t) = -\partial\mathbf{A}(t)/\partial t$ the electric field with amplitude $E_0$, $\Omega$ the light's frequency, and $A = E_0/\Omega$. The gauge potential is periodic in time, $A(t+T) = A(t)$, with period $T = 2\pi/\Omega$ and $l = 1(-1)$, stands for the right (left) polarization of the light. Equation (1) can be treated by the Floquet method with the aid of an effective static Hamiltonian [20] and leads to results that agree well with experiments [23, 24]. This formalism has been successfully applied to graphene [29] and disordered TIs [30]. For high frequencies $\Omega \gg ev_FE_0/\hbar\Omega$ and low intensities ($ev_FA \ll \hbar\Omega$) it gives the effective static Hamiltonian

$$H_l^s = v_F(\sigma_x p_y - \sigma_y p_x) + s\Delta_h\sigma_z + l\Delta_\Omega\sigma_z, \qquad (2)$$

where $\Delta_\Omega = e^2 v_F^2 \hbar^2 A^2/\hbar^3\Omega^3$ is the mass term induced by the off-resonant light. It breaks the time-reversal symmetry and its values are in the range of 100 meV [23, 24]. The diagonalization of Eq. (2) gives the eigenvalues

$$E_l^{s\lambda} = \lambda \left[\varepsilon_k^2 + \delta_{sl}^2\right]^{1/2} \tag{3}$$

and the corresponding eigenfunctions

$$\Psi_l^{s,\lambda} = (1/\sqrt{S}) \exp[i\mathbf{k}\cdot\mathbf{r}] \begin{pmatrix} i\varepsilon_k e^{-i\varphi}/Y \\ X/Y \end{pmatrix}. \tag{4}$$

Here $S = L_x L_y$, $\lambda = \pm 1$, $\varepsilon_k = v_F\hbar k$, $\delta_{sl} = l\Delta_\Omega + s\Delta_h$, $Y^2 = \varepsilon_k^2 + X^2$, $X = E_l^{s,\lambda} - \delta_{s,l}$, $\tan\varphi = k_y/k_x$, and $k^2 = k_x^2 + k_y^2$. We show the eigenvalues given by Eq. (3) in Fig. 1 for the symmetric (solid curves) and antisymmetric (dashed curves) states. We fixed the hybridization energy to 35 meV corresponding to 4 quintuple layers [3], $v_F = 0.5\times 10^6$ m/s, $a = 4.14$ Å , $\hbar\Omega = 8J = 8$ eV ($J$ is the nearest neighbor hopping amplitude), $\Delta_\Omega = 20$ meV ($ev_F A = 0.4$ eV) [20]. We find a well resolved gap between the valence and conduction bands and notice that the surfaces are nondegenerate if $\Delta_\Omega \neq 0$ and $\Delta_h \neq 0$. Here we vary the amplitude of the circularly polarized *off-resonant light* such that $\Delta_\Omega = 0$ meV, 20 meV, 35 meV ($ev_F A = 0.53$ eV), and 100 meV ($ev_F A = 0.9$ eV), which can be achieved by existing experimental techniques [23, 24]. As $\Delta_\Omega$ at $k = 0$ changes sign when the light polarization is reversed. The realization of this reversed state of the system upon changing the light polarization from right to left is an entirely new phenomenon; it is made clear upon contrasting Fig. 2 with Fig. 1.

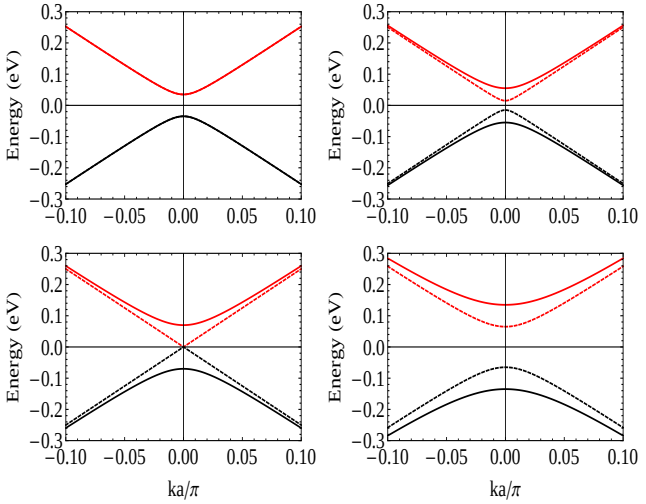


FIG. 1. Band structure for right-polarized light ($l = +1$). Here $\Delta_h = 35$ meV and $\Delta_\Omega = 0$ meV (top left), 20 meV (top right), 35 meV (bottom left), and 100 meV (bottom right). The solid (dashed) curves correspond to the symmetric (antisymmetric) surface states. Red and black colours represent the conduction and valence bands, respectively.

*Orbital magnetization.* The orbital magnetization of Bloch electrons has been a very attractive problem since the prediction and observation of its dependence on the Berry-curvature [13, 14]. To study thermoelectric transport properties we must include their temperature dependence. We obtain the equilibrium magnetization density from the free energy $F$ in a weak magnetic field $B$ ($B$ only couples to the orbital motion of electrons but does not contribute to the Zeeman energy [14]) written as

$$F = -\frac{1}{\beta}\sum_{s\lambda\mathbf{k}} \ln\left(1 + e^{\beta(\mu - E_{l\mathbf{k}}^{s\lambda})}\right). \tag{5}$$

Here $\beta = 1/k_B T$, $k_B$ is the Boltzmann constant, $T$ the temperature, and $\mu$ the chemical potential. Further, the electron energy $E_{l\mathbf{k}}^{s\lambda} = E_l^{s\lambda} - \mathbf{m}(\mathbf{k})\cdot\mathbf{B}$ includes a correction due to the orbital magnetic moment $\mathbf{m}(\mathbf{k}) = (-ie/2\hbar)\left\langle \nabla_k \Psi_l^{s\lambda} \right| \times [\hat{H} - E_l^{s\lambda}] \nabla_k \left| \Psi_l^{s\lambda} \right\rangle$.

To evaluate the sum over $\mathbf{k}$ in Eq. (5) we convert it to an integral and use the prescription $\sum_\mathbf{k} \to (1/2\pi)^2 \int d^2\mathbf{k}(1 + e\Omega(\mathbf{k})\cdot\mathbf{B}/\hbar)$, where $\Omega(\mathbf{k}) = \nabla_k \times \left\langle \Psi_l^s \right| i\nabla_k \left| \Psi_l^{s\lambda} \right\rangle$ is the Berry-curvature, see Ref. 14 for a detailed justification. The orbital magnetization $M_{orb} = M_c + M_\Omega$ is given by $M_{orb} = -(\partial F/\partial B)_{\mu,T}$. $M_c$ is the conventional term and $M_\Omega$ the additional term due to the Berry curvature. It originates from the self-rotation of the electron wave packet around its center of mass [14]. The results for $M_c$ and $M_\Omega$ are

$$M_c = (1/2\pi)^2 \sum_{s\lambda} \int m(\mathbf{k}) f(\mathbf{k})\, d^2k, \tag{6}$$

$$M_\Omega = (e/2\pi\beta h) \sum_{s\lambda} \int \Omega(\mathbf{k}) \ln\left(1 + e^{\beta(\mu - E_{l\mathbf{k}}^{s\lambda})}\right) d^2k, \tag{7}$$

with $f(\mathbf{k})$ the Fermi function. Equations (3) and (4) give

$$\Omega(\mathbf{k}) = (\hbar^2 v_F^2/2)\, \delta_{sl} / \left(\varepsilon_k^2 + \delta_{sl}^2\right)^{3/2}. \tag{8}$$

For finite $\Delta_h$ or $\Delta_\Omega$ the moment $m(\mathbf{k})$ has a peak at $k = 0$. For $\Delta_\Omega = 0$ and $\Delta_h = 35$ meV we obtain $m(\mathbf{k}) = 25$ Bohr magnetons. This value may be changed by varying the light intensity $\Delta_\Omega$. Then only the purely Berry-curvature-mediated orbital magnetization survives. For a qualitative analysis we obtain $M_{orb}$ at $T = 0$ and $\mu$ in the conduction band, as

$$M_{orb} = (e\mu/2h) \sum_s \left[1 - \delta_{sl}/\left(\varepsilon_{k_F}^2 + \delta_{sl}^2\right)^{1/2}\right]. \tag{9}$$

We show $M_{orb}$, obtained numerically from Eqs. (6) and (7), in Fig. 3. Its magnitude can be enhanced by tuning the band gap upon varying $\Delta_\Omega$ and/or $\mu$. As a reference, for $\mu = 100$ meV and a typical layer thickness $d$ of 2 nm, Eq. (9) gives $M_{orb} = 0.004$ T. The value of $M_c$, evaluated in the manner of Ref. 31, is one order of magnitude smaller than the $M_{orb}$. Magnetization values as small as 10 mT have been recently measured in a Cr-doped $Bi_2(Se, Te)_3$ TI [32]. The weak cusps at $\mu = \pm 45$ meV and $\pm 115$ meV are due to the gap induced by $\Delta_\Omega$ and $\Delta_h$; they are washed out as we raise the temperature to

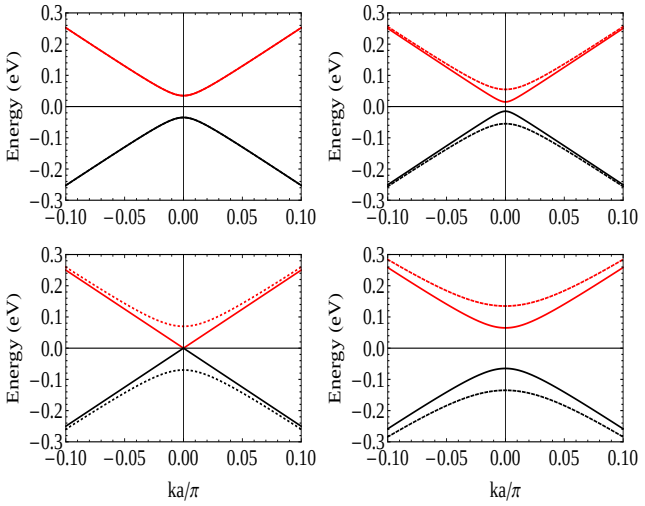


FIG. 2. As in Fig. 1 for left-polarized light ($l = -1$). All other parameters are the same as in Fig. 1

150 K (dotted). Notice though that the temperature dependence is weak. The orbital magnetization induced by *off-resonant light* can be distinguished from other sources of magnetization that don't depend on the polarization of light, e.g., from the one induced by spin-orbit coupling [33]. We can clearly see from Eq. (9) that $M_{orb}$ changes sign due to $l\Delta_\Omega$, for $\Delta_\Omega > \Delta_h$, when we reverse the light's polarization ($l = \pm 1$). This could be observed in experiments similar to those on magnetization [15] or by the Faraday-Kerr effect [34]. Moreover, very recently magnetization signatures of the off-resonant light effects on graphene have been simulated and helical edge states have been reported [35].

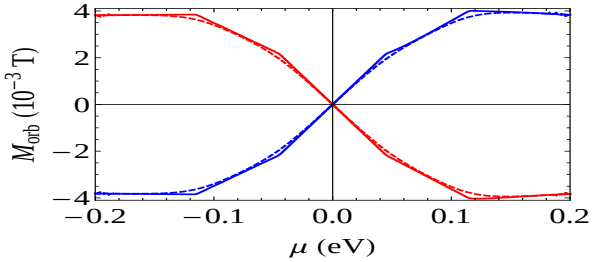


FIG. 3. $M_{orb}$ divided by the layer thickness (2 nm) vs $\mu$ for $T = 10$ K (solid) and 150 K (dotted). Here $\Delta_h = 35$ meV and $\Delta_\Omega = 80$ meV. Blue and red curves correspond to right- ($l = +1$) and left- ($l = -1$) polarized light, respectively.

*Thermal and Nernst conductivities.* The orbital magnetization contains a conventional contribution, Eq. (6), and a Berry-curvature-mediated one, Eq. (7). The relation between it and the Nernst conductivity, demonstrated in Refs. 13 and 14, shows that the conventional part does not contribute to the transport current whereas the Berry-curvature term directly does and modifies the intrinsic Hall current, obtained by an integral with respect to momentum, of the Berry curvature over the 2D Brillouin zone. The difference between the Hall $\sigma_{xy}$ and Nernst $\alpha_{xy}$ conductivities is that $\alpha_{xy}$ is determined not only by the Berry curvature but also by entropy generation around the Fermi surface. Therefore, $\alpha_{xy}$ is sensitive to changes of the Fermi energy and temperature. The heat current under a weak electric field $\mathbf{E}$ and a thermal gradient $\nabla T$ is given by $\mathbf{J}^Q = T\alpha \cdot \mathbf{E} - \kappa \cdot \boldsymbol{\nabla} T$. In this case the intrinsic Hall current is $j_x = -\alpha_{xy}\nabla_y T$ [11, 14]. With $\Omega \equiv \Omega(\mathbf{k})$ the component $\alpha_{xy}$ is given by

$$\alpha_{xy} = c\sum_{\mathbf{s}\lambda}\int \Omega\big[E_l^{s\lambda}(\mathbf{k}) f_{l\mathbf{k}}^{s\lambda} + k_B T \ln(1 - f_{l\mathbf{k}}^{s\lambda})\big] d^2k, \quad (10)$$

with $c = e/2\pi hT$, $f_{l\mathbf{k}}^{s\lambda} = f(E_l^{s\lambda}(\mathbf{k}))$ the Fermi-Dirac function, and $\mu$ the chemical potential. Recent experiments on graphene [36] agree well with Eq. (10). The component $\kappa_{xy}$ of the thermal conductivity tensor $\kappa$ reads

$$\kappa_{xy} = b\sum_{\mathbf{s}\lambda}\int d^2k\,\Omega\Big[\,\beta^2(E_l^{s\lambda})^2 f_{l\mathbf{k}}^{s\lambda} - 2\mathrm{Li}_2(1 - f_{l\mathbf{k}}^{s\lambda}) + \pi^2/3 - \log^2\left(1 + e^{-\beta E_l^{s\lambda}}\right)\Big], \quad (11)$$

where $b = ek_B/4\pi^2\beta h$; $\mathrm{Li}_2(x)$ is the polylogarithm function. Equations (10) and (11) can be simplified in the limit of low temperatures using the Mott relations [11, 14], $\alpha_{xy} = -(\pi^2 k_B^2 T/3e)(d\sigma_{xy}/d\mu) = -(e/k_B)d\kappa_{xy}/d\mu$ and $\kappa_{xy} = (\pi^2 k_B^2 T/3e^2)\sigma_{xy}$ with $\sigma_{xy}$ given by

$$\sigma_{xy} = \frac{e^2}{2\pi h}\sum_s \int \Omega\big(f_{l\mathbf{k}}^{s1} - f_{l\mathbf{k}}^{s,-1}\big)\, d^2k \quad (12)$$

For $T = 0$ and $\mu$ in the band gap Eq. (12) gives $\sigma_{xy}^0$, the Hall conductivity in the gap, as $\sigma_{xy}^0 = -(e^2/2h)sgn(\delta_{sl})$. Here it is interesting to note that for $\Delta_\Omega < \Delta_h$ the insulating state is trivial whereas for $\Delta_\Omega > \Delta_h$ the state is topological nontrivial; a topological phase transition occurs at $\Delta_\Omega = \Delta_h$. Such transitions were also reported in previous studies without off-resonant light [26–28, 37]. For $\mu$ in the conduction band we have $\sigma_{xy} \equiv \sigma_{xy}^c$ with

$$\sigma_{xy}^c = (e^2/2h)\sum_s \left[1 - \delta_{sl}/\left(\varepsilon_{k_F}^2 + \delta_{sl}^2\right)^{1/2}\right] \quad (13)$$

Notice that due to $\delta_{sl} = l\Delta_\Omega + s\Delta_h$ the sign of $\sigma_{xy}^c$ can be reversed, for $\Delta_\Omega > \Delta_h$, upon reversing the light polarization ($l \to -l$). Similar results can be obtained when the chemical potential $\mu$ is in the valence band due to symmetry. For a qualitative analysis we use Eq. (13) and obtain $\alpha_{xy}$, at very low temperatures, as

$$\alpha_{xy} = -(\pi^2\, ek_B^2 T/6h)\sum_s \delta_{sl}/\left(\varepsilon_{k_F}^2 + \delta_{sl}^2\right) \quad (14)$$

with $\mu$ in the conduction band; $\alpha_{xy}$ vanishes when $\mu$ is in the band gap. Thermoelectric transport can be understood by results such as Eq. (14) and agree well with low-temperature data [16–19, 36] from gapless graphene in a transverse magnetic field. The Nernst effect discussed here exists even without an external magnetic field, being solely driven by the weak $B$ field and the

Berry-curvature. Note that Eq. (10) is more general than Eq. (14) since it is valid beyond the $T \to 0$ regime.

The dependence of $\alpha_{xy}$ on the gate voltage (or chemical potential $\mu$) can be assessed by controlling the band gap, which has been realized experimentally in graphene [16–19, 36]. An enhanced thermoelectric response is achieved when the bands come close to the Dirac point. In Fig. 4 we show numerical results for $\alpha_{xy}$, given by Eq. (10), as a function of $\mu$ at $T = 100$ K (left) and $T = 200$ K (right). We use $\Delta_h = 0$ meV and vary the band gap by off-resonant light such that $\Delta_\Omega = 20$ meV (solid), $\Delta_\Omega = 70$ meV (dotted), and $\Delta_\Omega = 120$ meV (dot-dashed). We obtain similar results for fixed $\Delta_\Omega = 0$ meV and variable $\Delta_h$ using values similar to those of experiments [3]. The highest peak value of $\alpha_{xy}$, near $y \approx 0.4$ in Fig. 4, is $0.4\, ek_B/h \approx 52$ nA/K. Our results show that a certain thickness or an off-resonant light can significantly affect transport in TIs at room temperature or even above. Figure 5 shows $\alpha_{xy}$ versus $\mu$ for $T = 100$ K (left) and

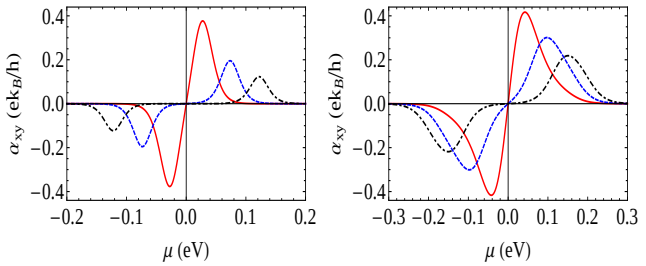


FIG. 4. Nernst conductivity vs $\mu$ for $T = 100$ K (left) and $T = 200$ K (right). Here $\Delta_h = 0$ meV, $l = +1$, and $\Delta_\Omega = 20$ meV (red solid), 70 meV (blue dashed), and 120 meV (black dot-dashed). We obtain similar results for $\Delta_\Omega$ and $\Delta_h$ interchanged.

$T = 200$ K (right), $\Delta_h = 35$ meV, and variable $\Delta_\Omega = 50$ meV (dotted blue), $\Delta_\Omega = 100$ meV (solid blue). The blue curve is for right polarization of the light whereas the black one is for left polarization. Each peak of Fig. 4 is split in two well separated peaks in both bands due to the combination of $\Delta_h \pm \Delta_\Omega$ for $T = 100$ K. This is consistent with Figs. 1 and 2. As we increase the temperature to 200 K or more, the splitting is suppressed but still persists till room temperature. We observe shifts of the peaks towards the Dirac point for decreasing $\Delta_\Omega$, which reflects the reduction of the band gap, and an increase of the amplitude. Notice how the sign of $\alpha_{xy}$ is reversed upon reversing the light polarization from right (blue, $l = +1$) to left (red, $l = -1$). This reversal corresponds to the exchange of the bands of the symmetric and antisymmetric surface states shown in Figs. 1 and 2. Thus, the transport can be tuned either by off-resonant light ($\Delta_\Omega$) or by the thickness ($\Delta_h$) of the TIs. This and the dependence of $\alpha_{xy}$ on the light polarization is, to our knowledge, an entirely new phenomenon.

In general, it depends on the sign of the Berry-curvature (cf. Fig. 1) whether the Nernst conductivity is positive or negative. Our results are valid for elevated temperatures in the experimentally relevant range [36]. Moreover, $\alpha_{xy} \neq 0$ when $\mu$ is in the band gap whereas

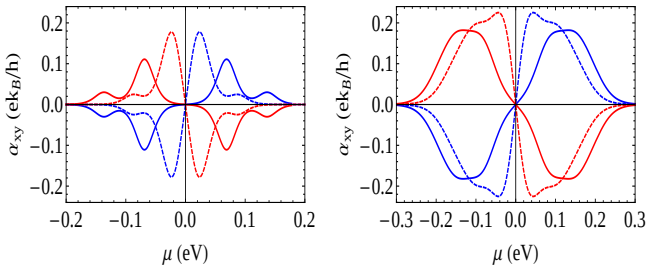


FIG. 5. Nernst conductivity vs $\mu$ for $T = 100$ K (left) and $T = 200$ K (right). Here $\Delta_h = 35$ meV and $\Delta_\Omega = 100$ meV (solid) and 50 meV (dotted). Blue and red curves correspond to right- ($l = +1$) and left- ($l = -1$) polarized light, respectively.

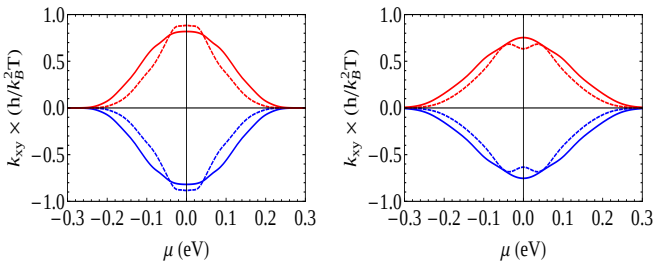


FIG. 6. Thermal conductivity vs $\mu$ for $T = 100$ K (left) and $T = 200$ K (right). Here $\Delta_h = 35$ meV and $\Delta_\Omega = 100$ meV (solid) and 50 meV (dotted). Blue and red curves correspond to right- ($l = +1$) and left- ($l = -1$) polarized light, respectively.

Eq. (14) yields $\alpha_{xy} = 0$ since it is the derivative of $\sigma^0_{xy}$, which is quantized and independent of $\mu$ in this case. Notice that given the Mott relations stated above Eq. (12), a similar sign reversal should occur in the thermal conductivity $\kappa_{xy}$ upon reversing the light polarization. Indeed, Fig. 6, in which we plot $\kappa_{xy}$ versus $\mu$, obtained numerically from Eq. (11), shows that this is the case: $\kappa_{xy}$ increases linearly with temperature. In contrast, $\sigma_{xy}$, given by Eq. (12), depends very weakly on temperature. The highest peak value of $\kappa_{xy}$, near $y \approx 1$ in Fig. 6, is $k_B^2 T/h \approx 1.2$ nAV/K. It is important to note that there may be additional contributions to thermoelectric transport properties due to phonons. However, these contributions are estimated to be negligible [11] for $T \sim 100$ K. This tuning of transport by an off-resonant light is pertinent to thermoelectric device applications. We believe that the $\kappa_{xy}$ and $\alpha_{xy}$ can be measured experimentally in a way similar to that used for bulk ferromagnet [38].

All our results, obtained within linear-response theory, rely on the assumption that the electronic subsystem is not far from thermal equilibrium when it is exposed to an external off-resonant light. This may not be obvious. However, as argued and explicitly demonstrated in Ref. 20 by the use of an adiabatic theorem for periodically-driven systems, the transport properties of the nonequilibrium systems are well approximated by those of the system described by an effective *static* Hamiltonian that incorporates virtual photon absorption processes. Moreover, using the Floquet Fermi golden rule [20], it has been demonstrated that excitations in the bands of effective

Hamiltonians still require a physical energy greater than the gap. It is in principle possible to absorb energies from photons, but because their frequency is assumed much larger than the bandwidth, such an absorption requires excitations of electrons and many phonons and, therefore, is suppressed. Accordingly, at low temperatures the insulating state of the effective Hamiltonian is protected against electron-phonon interactions by the gap. This holds for short laser pulses and was fulfilled in recent experiments [23, 24]. Also, due to its topological nature, the effect we obtain should generally be stable against imperfections of the sample.

*Summary.* We evaluated analyticaly and numerically the band structure and thermoelectric transport properties of ultrathin TIs under the application of *off-resonant light*. We showed that by applying a circularly polarized light, the band gap is tuned and results in enhanced thermoelectric transport. Moreover, changing the light polarization from right to left leads to an exchange of the conduction and valence bands of the symmetric and antisymmetric surface states and to a sign reversal of the Nernst and thermal conductivities and of the Berry-curvature-induced orbital magnetization. The results present new opportunities for state-exchanged excitations under light and tunable thermoelectric transport properties.

Our work was supported by the Canadian NSERC Grant No. OGP0121756.

†Electronic address: m.tahir06@alumni.imperial.ac.uk
⋆Electronic address: p.vasilopoulos@concordia.ca

[1] M. Z. Hasan and C. L. Kane, Rev. Mod. Phys. **82** , 3045 (2010); X. L. Qi and S. C. Zhang, *ibid* **83**, 1057 (2011); J. E. Moore, Nature **464**, 194 (2010).
[2] H. Zhang, C.-X. Liu, X.-L. Qi, X. Dai, Z. Fang, and S.-C. Zhang, Nature Phys. **5**, 438 (2009).
[3] Y. Zhang, K. He, C. Z. Chang, C. L. Song, L. L. Wang, X. Chen, J. F. Jia, Z. Fang, X. Dai, W. Y. Shan, S. Q. Shen, Q. Niu, X. L. Qi, S. C. Zhang, X. C. Ma, and Q. K. Xue, Nature Phys. **6**, 584 (2010).
[4] S. Chadov, X.-L. Qi, J. K̈ubler, G. H. Fecher, and C. F. S.-C. Zhang, Nature Material **9**, 541 (2010).
[5] H. Lin, L. A. Wray, Y. Xia, S. Xu, S. Jia, R. J. Cava, A. Bansil, and M. Z. Hasan, Nature Material **9**, 546 (2010).
[6] X. Zhang, H. Zhang, J. Wang, C. Felser, and S.-C. Zhang, Science **335**, 1464 (2012).
[7] X. Zhang, J. Wang, and S.-C. Zhang, Phys. Rev. B **82**, 245107 (2010).
[8] S. Cho, N.P. Butch, J. Paglione, and M. S. Fuhrer, Nano Lett. **11**, 1925 (2011).
[9] H. Peng, W. Dang, J. Cao, Y. Chen, D. Wu, W. Zheng, H. Li, Z.-X. Shen, and Z. Liu, Nature Chem. **4**, 281 (2012).
[10] P. Ghaemi, R. S. K. Mong, and J. E. Moore, Phys. Rev. Lett. **105**, 166603 (2010).
[11] T. Yokoyama and S. Murakami, Phys. Rev. B **83**, 161407(R) (2011).
[12] K. Uchida, S. Takahashi, K. Harii, J. Ieda, W. Koshibae, K. Ando, S. Maekawa, and E. Saitoh, Nature **455**, 778 (2008).
[13] D. Xiao, Y. Yao, Z. Fang, and Q. Niu, Phys. Rev. Lett. **97**, 026603 (2006).
[14] D. Xiao, M. C. Chang, and Q. Niu, Rev. Mod. Phys. **82**, 1959 (2010).
[15] S. Y. Xu, M. Neupane, C. Liu, D. Zhang, A. Richardella, L. A. Wray, N. Alidoust, M. Leandersson, T. Balasubramanian, J. S. Barriga, O. Rader, G. Landolt, B. Slomski, J. H. Dil, J. Osterwalder, T. R. Chang, H. T. Jeng, H. Lin, A. Bansil, N. Samarth, and M. Z. Hasan, Nature Phys. **8**, 616 (2012).
[16] P. Wei, W. Bao, Y. Pu, C. N. Lau, and J. Shi, Phys. Rev. Lett. **102**, 166808 (2009).
[17] Y. M. Zuev, W. Chang, and P. Kim, Phys. Rev. Lett. **102**, 096807 (2009).
[18] K. L. Grosse, M.-H. Bae, F. Lian, E. Pop, and W. P. King, Nature Nanotechnol. **6**, 287 (2011).
[19] A. A. Balandin, Nature Material **10**, 569 (2011).
[20] T. Kitagawa, T. Oka, A. Brataas, L. Fu, and E. Demler, Phys. Rev. B **84**, 235108 (2011).
[21] N. H. Lindner, G. Refael, and V. Galitski, Nature Physics **7**, 490 (2011); N. H. Lindner, D. L. Bergman, G. Refael, and V. Galitski, Phys. Rev. B **87**, 235131 (2013).
[22] M. C. Rechtsman, J. M. Zeuner, Y. Plotnik, Y. Lumer, D. Podolsky, F. Dreisow, S. Nolte, M. Segev, and A. Szameit, Nature **496**, 196 (2013).
[23] Y. H. Wang, H. Steinberg, P. J. Herrero, and N. Gedik, Science **342**, 453 (2013).
[24] H. Zhang, J. Yao, J. Shao, H. Li, S. Li, D. Bao, C. Wang, and G. Yang, Sci. Rep. **4**, 5876 (2014).
[25] D. K. Efimkin and Yu. E. Lozovik, Phys. Rev. B **87**, 245416 (2013); Z. Li and J. P. Carbotte, *ibid* **88**, 045414 (2013); M. Lasia and L. Brey, *ibid* **90**, 075417 (2014).
[26] H.-Z. Lu, W.-Y. Shan, W. Yao, Q. Niu, and S.-Q. Shen, Phys. Rev. B **81**, 115407 (2010).
[27] J. Linder, T. Yokoyama, and A. Sudbo, Phys. Rev. B **80**, 205401 (2009).
[28] C.-X. Liu, H. Zhang, B. Yan, X.-L. Qi, T. Frauenheim, X. Dai, Z. Fang, and S.-C. Zhang, Phys. Rev. B **81**, 041307 (2010).
[29] Á. Gómez-León, P. Delplace, and G. Platero, Phys. Rev. B **89**, 205408 (2014).
[30] P. Titum, N. H. Lindner, M. C. Rechtsman, and G. Refael, arXiv:1403.0592v1.
[31] D. Xiao, W. Yao, and Q. Niu, Phys. Rev. Lett. **99**, 236809 (2007).
[32] L. J. Collins-McIntyre, S. E. Harrison, P. Scho?nherr, N.-J. Steinke, C. J. Kinane, T. R. Charlton, D. Alba-Veneroa, A. Pushp, A. J. Kellock, S. S. P. Parkin, J. S. Harris, S. Langridge, G. van der Laan, and T. Hesjedal, EuroPhys. Lett., **107**, 57009 (2014).
[33] M. M. Grujić, M. Z. Tadić, and F. M. Peeters, Phys. Rev. B **90**, 205408 (2014).
[34] Y. K. Kato, R. C. Myers, A. C. Gossard, and D. D. Awschalom, Science **306**, 1910 (2004).
[35] J. P. Dahlhaus, B. M. Fregoso, and J. E. Moore, arXiv:1408.6811v1.
[36] J. G. Checkelsky and N. P. Ong, Phys. Rev. B **80**, 081413

(2009).
[37] B. Seradjeh, J. E. Moore, and M. Franz, Phys. Rev. Lett. **103**, 066402 (2009).
[38] Wei-Li Lee, S. Watauchi, V. L. Miller, R. J. Cava, and N. P. Ong, Phys. Rev. Lett. **93**, 226601 (2004).